



Imaging Cancer Cells Expressing the Folate Receptor with Carbon Dots Produced from Folic Acid

Susanta Kumar Bhunia,^[a] Amit Ranjan Maity,^[b] Sukhendu Nandi,^[a] David Stepensky,^[b] and Raz Jelinek^{*[a, c]}

Development of new imaging tools for cancer cells in vitro and in vitro is important for advancing cancer research, elucidating drug effects upon cancer cells, and studying cellular processes. We showed that fluorescent carbon dots (C-dots) synthesized from folic acid can serve as an effective vehicle for imaging cancer cells expressing the folate receptor on their surface. The C-dots, synthesized through a simple one-step process from folic acid as the carbon source, exhibited selectivity towards cancer cells displaying the folate receptor, making

such cells easily distinguishable in fluorescence microscopy imaging. Biophysical measurements and competition experiments both confirmed the specific targeting and enhanced uptake of C-dots by the folate receptor-expressing cells. The folic acid-derived C-dots were not cytotoxic, and their use in bioimaging applications could aid biological studies of cancer cells, identification of agonists/antagonists, and cancer diagnostics.

Introduction

Specific staining of cancer cells is an important goal in cancer research, as it enables direct investigation of cell biology, varied cellular processes, and the effects of therapeutic treatments.^[1] Intensive efforts have been directed towards development of chemical compounds that would target and selectively label cancer cells.^[2] Fluorescent dyes, in particular, have been widely used as vehicles for cell labeling.^[3,4] Fluorescent semiconductor nanoparticles (often termed quantum dots), have also been extensively used in recent years for cell labeling.^[5] Quantum dots, however, comprise cell-toxic elements (such as cadmium and arsenic) in many instances and usually require functionalization designed to make the particles biocompatible.^[6]

Another notable challenge for employing fluorescent dyes and nanoparticles for cell labeling is to accomplish cell specificity. Means for cell targeting have generally focused on modification of the fluorescent markers with recognition elements and ligands designed to bind on cell-surface receptors.^[7] The folate receptor, in particular, overexpressed on the surface of different types of cancer cells,^[7–9] has been employed as a docking site for both therapeutic agents and fluorescent dyes.^[7,10]

Folate (or its acid form, folic acid) is essential for all cell functioning, and this metabolite is found in high levels in many cancer cells. Accordingly, folic acid was conjugated to varied dyes and fluorescent nanoparticles and used for imaging of cancer cells.^[5,9,11–13] However, the construction of folic acid-coupled labels often involves demanding synthetic processes that often exhibit low reaction yields.

Carbon dots (C-dots) constitute newly discovered fluorescent nanoparticles exhibiting great promise as bioimaging agents. C-dots are quasi-spherical nanoscale (< 10 nm) particles^[14] and have attracted significant research interest due to their unique structural and photophysical properties and applications in nano-biotechnology.^[15] C-dots are particularly advantageous for biological applications, as they are biocompatible and potentially less cytotoxic than semiconductor quantum dots. Moreover, C-dots are chemically stable and display broad excitation/emission spectral ranges and low photobleaching, which are favorable characteristics for bioimaging applications.^[16,17] A particularly attracting property of C-dots has been the observation that they can be produced from a wide variety of carbon sources, providing the means to modulate their structural properties.^[16–27] We have recently synthesized C-dots that are covalently linked to hydrocarbon chains and demonstrated their use for cell imaging applications.^[15,18] C-dots were previously coupled to folic acid and employed as conduits for cell labeling,^[12,16] however, as indicated above, such synthetic schemes are chemically elaborate.

Here, we present a simple strategy for construction of fluorescent C-dots that target cancer cells through the use of *folic acid* as the carbon source in C-dot synthesis. The C-dots were synthesized in a simple single-step process without conjugating folic acid with the prepared C-dots, as pursued in previous studies.^[12] We showed that the folic acid-derived C-dots could

[a] Dr. S. K. Bhunia, Dr. S. Nandi, Prof. R. Jelinek
Department of Chemistry, Ben-Gurion University of the Negev
Beer Sheva 84105 (Israel)
E-mail: razj@bgu.ac.il

[b] Dr. A. R. Maity, Dr. D. Stepensky
Department of Clinical Biochemistry and Pharmacology
The Faculty of Health Sciences, Ben-Gurion University of the Negev
Beer Sheva 84105 (Israel)

[c] Prof. R. Jelinek
Ilse Katz Institute for Nanotechnology, Ben-Gurion University of the Negev
Beer Sheva 84105 (Israel)

Supporting information for this article is available on the WWW under <http://dx.doi.org/10.1002/cbic.201500694>.

selectively stain folate receptor-expressing cancer cells by targeting the folate receptors on the cell surfaces. Indeed, quantitative analysis confirmed the direct relationship between the extent of cell labeling and the abundance of folate receptors. We demonstrated that the newly designed C-dots could facilitate identification of agonists/antagonists for the folate receptor, thus aiding the development of new cancer therapeutics.

Results and Discussion

Synthesis and characterization

The C-dots were prepared by a simple one-step synthetic route in which folic acid was mixed with NaOH and heated to 90 °C to induce carbonization (Figure 1A). Synthesis was carried out under basic conditions, as folic acid is sparingly soluble at acidic pH levels. During the carbonization process, the reaction mixture changed color from pale yellow to brown and eventually to dark brown, indicating the formation of carbon dots. Statistical analysis of particle sizes extracted from transmission electron microscopy (TEM) data in Figure 1B indicated that the synthesized C-dots exhibited a narrow size distribution at approximately 3.5 ± 0.6 nm. A high-resolution TEM (HR-TEM) image (Figure 1C) underscored the crystalline graphitic organization of the C-dots, displaying an in-plane lattice spacing of 0.215 nm, corresponding to the [110] planes of graphite.^[28] Raman scattering data corroborated the presence of graphitic

carbon as the most prominent component of the C-dots (Figure S1 in the Supporting Information).

The spectroscopic data in Figure 1E and F further illuminate the C-dots' structural and photophysical properties. The ultraviolet-visible absorption spectrum of the C-dots (after separation from the reaction mixture and removal of unreacted substances) features a strong peak around 280 nm, corresponding to the π - π^* transition of the aromatic sp^2 carbons within the C-dots' core. Importantly, the shoulder at approximately 360 nm was ascribed to folic acid residues that were not carbonized and displayed upon the C-dots' surface.^[16] The excitation-dependent emission spectra in Figure 1F indicate that, unlike most C-dot systems reported thus far, the emission peak remained at a constant wavelength of ~ 450 nm and did not shift upon excitation at different wavelengths. The absence of excitation-dependent emission shifts, depicted in Figure 1F, might be attributed to a relative uniformity of surface functionalization, resulting in narrow distribution of surface energy states.^[29,30] Figure 1F also shows that the highest luminescence intensity was recorded upon excitation at 365 nm; a fluorescent quantum yield of 9% was calculated with respect to quinine sulfate as a standard. The excitation-dependent emission spectra were independent of the solution pH (Figure S2).

X-ray photoelectron spectroscopy (XPS) analysis (Figure 2) illuminated the different functional groups displayed upon the C-dots' surface. Corroborating the reaction Scheme in Figure 1A, the raw XPS data (Figure 2A) depicted peaks corresponding to carbon, nitrogen, and oxygen. The carbon 1S spectrum in Figure 2B showed peaks at 284.8 and 287.4 eV, corresponding to C=C and C-OH groups, respectively.^[16] In the case of nitrogen, a peak at 399.3 eV for C-N and/or C=N groups was recorded, and another signal at 400.2 eV corresponded to the N-O group (Figure 2C). The oxygen 1S spectrum in Figure 2D revealed a peak at 531.2 eV, attributed to the C=O group, and at 532.2 eV for O=C-OH and/or C-OH groups (Figure 2D). Fourier-transform infrared (FTIR) analysis similarly showed the presence of different carbon-bonded, nitrogen-bonded, and oxygen-bonded units arising from the synthesis pathway utilizing folic acid as the reagent for C-dot formation (Figure S3).

The colloidal stability of the synthesized C-dots under physiological conditions was assessed. The results (Figure S2) indicated that the C-dots were stable for weeks without undergoing precipitation and degradation. Luminescence analysis pointed to very low photobleaching (Figure S4). These properties underscore the potential for using folic acid-derived C-dots in biological studies.

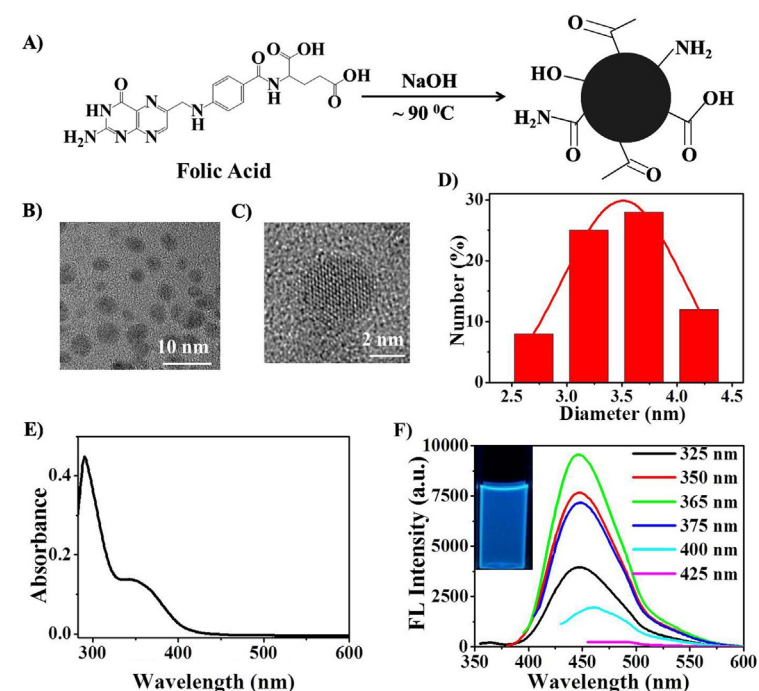


Figure 1. Carbon dot synthesis from folic acid and characterization. A) Scheme depicting one-step synthesis of the C-dots. B) Transmission electron microscopy (TEM) imaging of the C-dots. C) High-resolution TEM (HR-TEM) image of a C-dot showing the [110] crystalline graphitic planes. D) Histogram depicting the size distribution of the C-dots, extracted from the TEM experiment. E) Ultraviolet-visible (UV/Vis) absorption spectrum of the C-dots in aqueous solution. F) Emission spectra recorded under different excitation wavelengths; the inset shows a digital image of the C-dot solution illuminated by a UV lamp.

Cell imaging

The objective of this study was to achieve specific microscopic imaging of cells displaying the folate receptor through incubation with newly designed C-dots, synthesized from folic acid as the carbon source

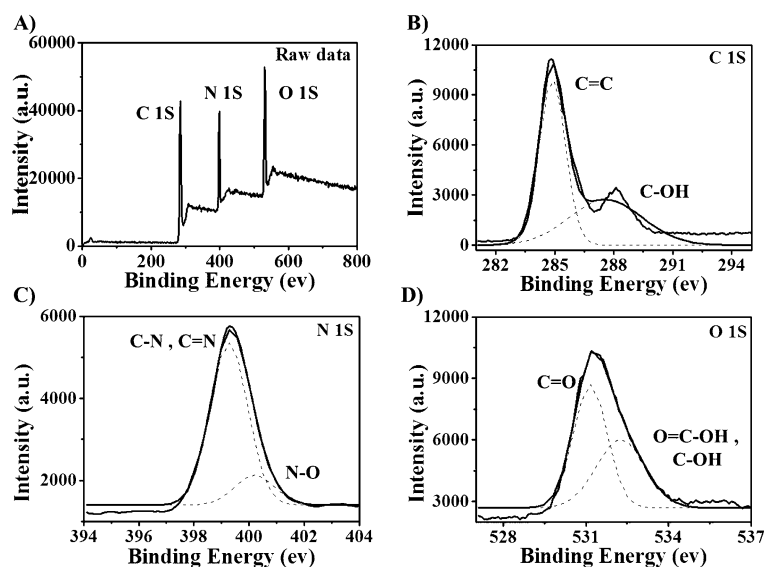


Figure 2. X-ray photoelectron spectroscopy (XPS) of the C-dots. A) XPS raw data showing the carbon, nitrogen, and oxygen elemental signatures. B) Deconvoluted C 1s spectrum. C) Deconvoluted N 1s spectrum. D) Deconvoluted O 1s spectrum.

(Figure 1A). Figures 3 and 4 show the results of fluorescence confocal microscopy experiments demonstrating application of the C-dots for selective imaging of cancer cells, depending upon the extent of folate receptor expression. The experiments depicted in Figure 3 examine the fluorescence labeling of representative cell lines exhibiting different degrees of folate receptor expression, following incubation with the folic acid-derived C-dots. Indeed, the fluorescence microscopy data in Figure 3A underscore the remarkable cell selectivity of the C-dots. Specifically, HeLa and SKOV3 cells, which overexpress the folate receptor,^[7–9] displayed the most pronounced fluorescence intensity, consistent with surface binding and uptake of the C-dots by the cells (Figure 3A, top). HepG2 and MCF7 cells, on the other hand, were fluorescently labeled to a lesser degree (Figure 3A, middle), and these cell lines exhibit medium or low folate receptor expression.^[8,31] Notably, CHO and A549 cells, which are deficient in folate receptor expression on their surface,^[5,9,32] were scarcely fluorescently labeled following incubation with the C-dots (Figure 3A, bottom).

The emission intensity plot in Figure 3B, which was calculated from the confocal cell images in Figure 3A, provided a quantitative measure for imaging specificity by the C-dots. As apparent in Figure 3B, the order of recorded fluorescence intensity indeed reflects the relative expression of the folate receptor by the cells, providing evidence that cell imaging is related to specific binding to the cells by the folic acid-derived C-dots. A quantitative analysis in which C-dot fluorescence was recorded following cell lysis (Figure S5A) gave rise to similar results, demonstrating a direct relationship between cell uptake of the fluorescent C-dots and the degree of folate receptor expression upon the cell surface.

To further confirm that the selective cell labeling apparent in Figure 3 was indeed directly related to production of the C-dots from folic acid, we also examined cell labeling by using C-dots that were prepared from different carbon sources

(Figure 4). Specifically, when we incubated HeLa cells with C-dots prepared from a 6-*O*-(*O*′-di-lauroyl-tartaryl)-*D*-glucose precursor^[15] or from arginine, significantly lower fluorescence intensities were observed in the confocal microscopy images (Figure 4B and C), which were also reflected in the corresponding emission intensity plot (Figure 4D). Similar results were obtained in the quantitative analysis by cell lysis (Figure S5). The lower fluorescence signals in Figure 4B and C were not related to variations in the quantum yield (The C-dots prepared from arginine and 6-*O*-(*O*′-di-lauroyl-tartaryl)-*D*-glucose precursor were found to exhibit quantum yields of 21 and 4.7%, respectively) but are rather indicative of lesser cell uptake of C-dots that were not prepared from folic acid. The fluorescence microscopy images in Figure 4A–C and the corresponding statistical analysis in Figure 4D clearly show that folate residues constitute the essential factor for cell targeting and uptake of the C-dots.

Figure 5 presents the results of a competition assay in which free folic acid was co-added to the cell medium. The data in Figure 5 nicely demonstrate the use of the C-dot labeling assay for evaluation of potential agonists/antagonists directed to the folate receptor. Specifically, the bar graph depicts the fluorescence intensity ($\lambda_{\text{ex}} = 365 \text{ nm}$; $\lambda_{\text{em}} = 450 \text{ nm}$) recorded when HeLa cells were first incubated with different concentrations of free folic acid, prior to addition of the folic acid-derived C-dots. Indeed, Figure 5 shows a pronounced inverse correlation between the extent of fluorescence emission signal and the concentration of free folic acid, that is, less staining of the HeLa cells with the C-dots was observed when higher concentrations of free folic acid were added.

A similar trend was apparent when a lower concentration of C-dots was used (Figure S6), or when the free folic acid and C-dots were mixed prior to addition to the cells (Figure S7). Importantly, no inhibition of cell staining was apparent when the cells were pre-incubated with glucose instead of folic acid (Fig-

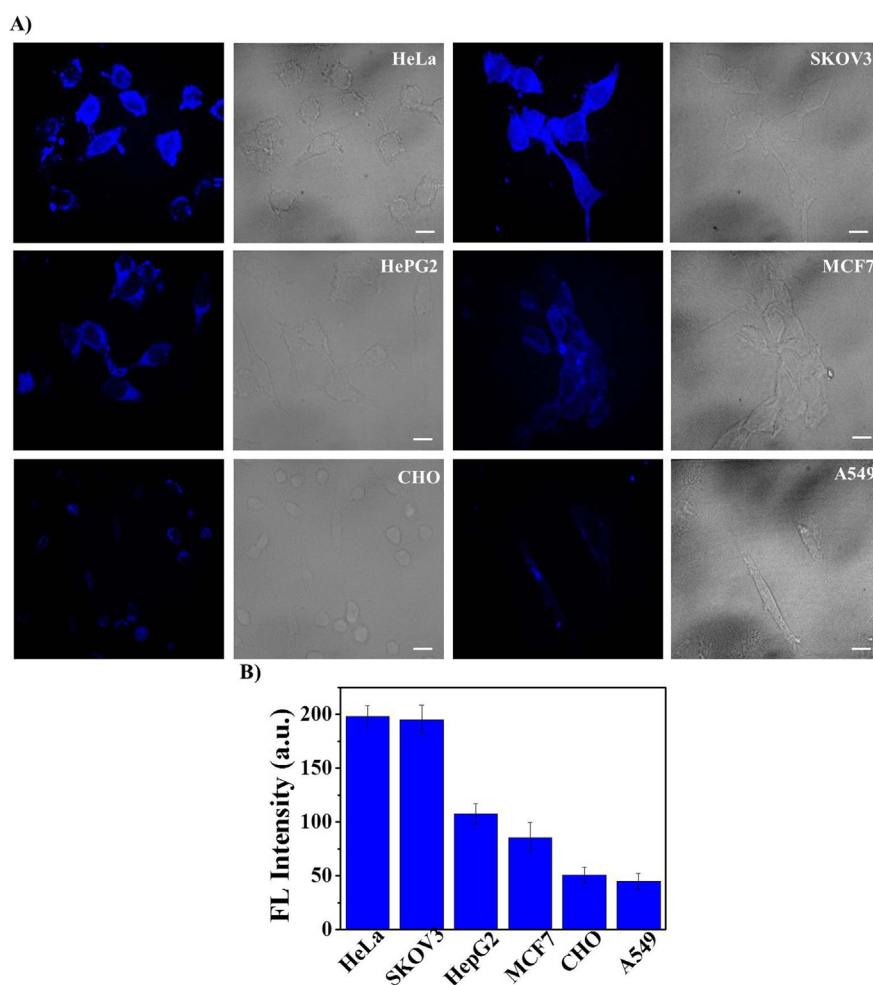


Figure 3. C-dots used for fluorescence microscopic imaging of cells expressing the folate receptor to different degrees. A) Confocal fluorescence microscopy images of different fix cells incubated with the folic-acid derived C-dots for 6 h. Left images correspond to fluorescence microscopy ($\lambda_{\text{ex}}=405$ nm, $\lambda_{\text{em}}=445/460$ nm), and right images correspond to bright-field images of the cells. Scale bar: 10 μm . B) Emission intensity plot calculated through summation of the fluorescence intensity associated with the cells.

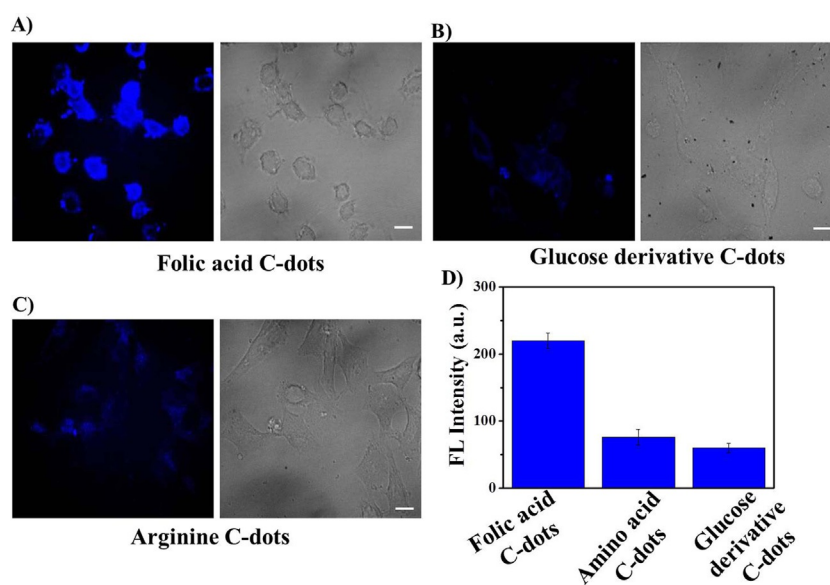


Figure 4. Cell labeling by using different types of C-dots. Confocal microscopy of fixed HeLa cells incubated with C-dots prepared from A) folic acid, B) arginine, and C) 6-*O*-(*O*-*O*'-di-lauroyl-tartaryl)-D-glucose precursor ($\lambda_{\text{ex}}=405$ nm, $\lambda_{\text{em}}=445/460$ nm). The bright field images are shown at right. Scale bar: 10 μm . D) Emission intensity plot calculated from the confocal microscopy images.

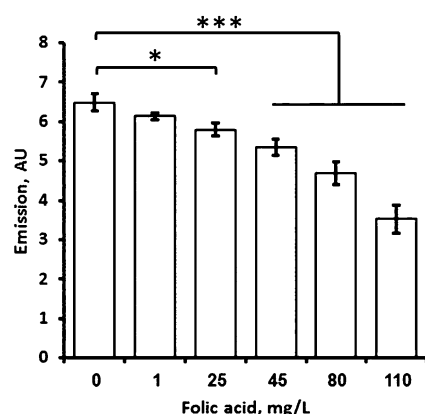


Figure 5. Folic acid competition assay. Fluorescence emission intensity ($\lambda_{\text{ex}} = 365 \text{ nm}$, $\lambda_{\text{em}} = 450 \text{ nm}$), recorded following incubation of the folic acid-derived C-dots with HeLa cells in media containing different concentrations of free folic acid. * $p < 0.05$, *** $p < 0.001$

ure S8), confirming that blocking of the folate receptor by free folic acid was the underlying reason for the reduction in fluorescence signals outlined in Figure 5.

An important advantage of C-dots over other cell staining substances currently in use (such as inorganic quantum dots) is their biocompatibility and low cytotoxicity. To assess the effect of the folic acid-derived C-dots upon cell viability, we carried out a 3-(4,5-dimethylthiazol-2-yl)-2,5-diphenyltetrazolium bromide (MTT) assay (Figure 6). The results of the MTT assay indicated that the C-dots exhibited low toxicity up to a substantial concentration (1.2 mg mL^{-1}). It should be noted that a much lower C-dots concentration of around 0.2 mg mL^{-1} was required for the cell imaging experiments depicted in Figures 3 and 4.

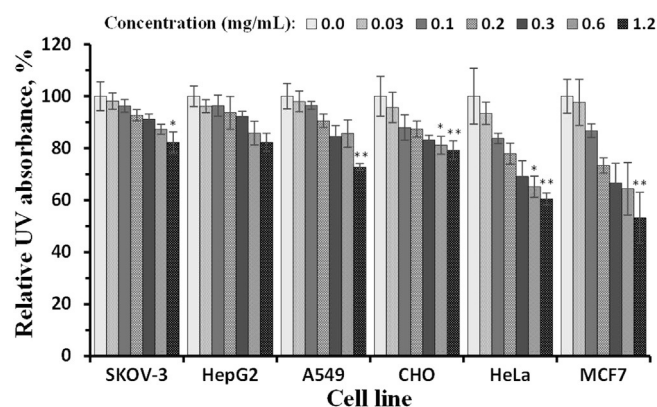


Figure 6. Cell viability in the presence of the C-dots. MTT cytotoxicity assay results. * $p < 0.05$ vs. the control (no carbon dots), ** $p < 0.01$ vs. the control (no carbon dots)

Conclusions

Selective imaging of cancer cells expressing the folate receptor on their surface was achieved by C-dots prepared from folic acid as the carbon source. The C-dots were synthesized in

a simple single-step process without conjugation of free folic acid; spectroscopic data confirmed the display of folic acid residues on their surface. Fluorescence microscopy and quantitative analyses demonstrated that the folic acid-derived C-dots effectively targeted cells expressing the folate receptor on their surface, thereby providing a means for selective microscopic imaging of cancer cells. Competition experiments further indicated potential use of the C-dot assay for assessing the activity of folate receptor agonists and antagonists. Of particular importance is that the folic acid-derived C-dots were not cytotoxic; this opens avenues for cancer cell imaging and analysis.

Experimental Section

Materials: Folic acid, dialysis tubing (benzoylated, MWCO ~ 2000 Da), RPMI-1640 folate free media, and methylthiazolyldiphenyltetrazolium bromide (MTT) were purchased from Sigma-Aldrich, and sodium hydroxide was purchased from Frutarom (Haifa, Israel). Fluoroshield solution was purchased from Immunobioscience (Mukilteo, WA).

Synthesis of carbon dots: Folic acid (100 mg) was mixed with water (5 mL), and sodium hydroxide solution (400 μL , 20 M) was added to the folic acid solution. The whole solution was then heated at $\sim 80\text{--}90^\circ\text{C}$ for 1.5 h. The resulting solution color was changed from light yellow to brown, indicating formation of carbon dots. The solution was dialyzed against water by using a dialysis membrane for purification of resulting carbon dots and removal of unreacted reagents.

Quantum yield measurement: The QYs of the samples were measured by using quinine sulfate as the reference (QY = 58% at $\lambda_{\text{ex}} = 340 \text{ nm}$).^[16] The formula used for QY measurement is as follows:

$$(\text{QY})_{\text{Sm}} = (\text{QY})_{\text{St}} \frac{(\text{PL}_{\text{area}}/\text{OD})_{\text{Sm}} \cdot \eta_{\text{St}}^2}{(\text{PL}_{\text{area}}/\text{OD})_{\text{St}} \cdot \eta_{\text{Sm}}^2}$$

in which Sm indicates the sample, St indicates the standard, η is the refractive index of the solvent, PL_{area} indicates the fluorescence area, and OD indicates the absorbance value.

Analytical methods: High-resolution transmission electron microscopy (HRTEM) samples were prepared by putting a drop of a nanoparticle solution on a graphene-coated copper grid and observing with a 200 kV JEOL JEM-2100F microscope. UV/visible absorption spectra of carbon dots in aqueous solutions were measured on a JASCO V-550 UV/visible spectrophotometer. Fluorescence emission spectra were recorded on a FL920 spectrofluorimeter and a Varioskan plate reader. X-ray photoelectron spectroscopy (XPS) of dried carbon dots was performed on an X-ray photoelectron spectrometer ESCALAB 250 ultrahigh vacuum (1×10^{-9} bar) apparatus with an Al K_{α} X-ray source and a monochromator. The X-ray beam size was 500 μm , survey spectra were recorded with pass energy (PE) 150 eV, and high-energy resolution spectra were recorded with PE 20 eV. The XPS results were processed with the AVANTGE program.

Cell experiments: Cells were plated in 24-well tissue culture plates on glass coverslips. After 24 h, a carbon dots solution (ca. 60 μL ; 2.5 mg mL^{-1}) at pH 7 was added to each well, and the cells were incubated for 6 h. The cells were subsequently washed with phosphate-buffered saline (PBS; 3 \times) times to completely remove un-

bound C-dots, fixed with 2.5% formaldehyde solution, followed by washing with PBS, and the cover slip was mounted on glass slides by using Fluoroshield solution.

For quantitative comparison analysis of cellular uptake of C-dots in different cell lines, cells were cultured in 24-well plates overnight. Then, 200 μL (2.5 mg mL^{-1}) samples were incubated for 6 h. Cells were washed carefully to remove excess sample. Cells were then treated with lysis buffer for 10 min to disrupt cell membranes and free the C-dots. Finally, emission spectra were measured.

For the competition assay of cellular uptake of C-dots in HeLa cells in the presence of different amount of folic acid in the cell culture medium, we cultured cells in RPMI medium containing varying amounts of folic acid (1–110 mg L^{-1}) for 24 h, then cells were seeded in 24-well plates overnight, and measurements were performed as done previously with different concentrations of C-dots.

For the glucose competition experiment, cells were cultured in RPMI medium with varying concentrations of free glucose (7–20 g L^{-1}) for 24 h and seeded in 24-well plates overnight, then measured by following the same procedure with a fixed concentration of C-dots.

For cytotoxicity studies, cells were incubated in 96-well plates with different concentrations of samples for 24 h. The cells were subsequently washed with PBS, followed by incubation with MTT solution for 1 h. The crystals were dissolved in DMSO, and absorbance was measured at 560 nm. The optical density was related to cell viability by assuming 100% viability for the control sample without C-dots.

Statistical analysis: All experiments were performed in triplicate, and the outcomes of one representative data set are reported. The data are presented as the mean \pm SD. Statistical differences in the studied parameters between the samples were analyzed by using ANOVA with the Tukey-Kramer post-test using Prism 5 software (GraphPad Software Inc.). *P* values less than 0.05 were considered significant.

Acknowledgements

S.K.B. and A.R.M. are grateful to the Planning and Budgeting Committee (PBC) of the Israeli Council for Higher Education for Outstanding Postdoctoral Fellowships. The Kreitman School of Advanced Graduate Studies is also acknowledged (S.N.).

Keywords: carbon dots • cell imaging • competition assays • folate receptor • folic acid

- [1] Y. Urano, D. Asanuma, Y. Hama, Y. Koyama, T. Barrett, M. Kamiya, T. Nagano, T. Watanabe, A. Hasegawa, P. L. Choyke, H. Kobayashi, *Nat. Med.* **2009**, *15*, 104–109.
[2] W. C. Silvers, B. Prasai, D. H. Burk, M. L. Brown, R. L. McCarley, *J. Am. Chem. Soc.* **2013**, *135*, 309–314.

- [3] D. Feng, Y. C. Song, W. Shi, X. H. Li, H. M. Ma, *Anal. Chem.* **2013**, *85*, 6530–6535.
[4] V. Ramu, F. Ali, N. Taye, B. Garai, A. Alam, S. Chattopadhyay, A. Das, *J. Mater. Chem. B* **2015**, *3*, 7177–7185.
[5] P. Suriamoorthy, X. Zhang, G. Hao, A. G. Joly, S. Singh, M. Hossu, X. Sun, W. Chen, *Cancer Nanotechnol.* **2010**, *1*, 19–28.
[6] I. L. Medintz, H. T. Uyeda, E. R. Goldman, H. Mattoussi, *Nat. Mater.* **2005**, *4*, 435–446.
[7] Z. Y. Wang, S. F. Zong, J. Yang, J. Li, Y. P. Cui, *Biosens. Bioelectron.* **2011**, *26*, 2883–2889.
[8] X. Ma, Y. Zhao, K. W. Ng, Y. L. Zhao, *Chem. Eur. J.* **2013**, *19*, 15593–15603.
[9] Y. Zheng, Z. Cai, X. R. Song, B. Yu, Y. Q. Bi, Q. H. Chen, D. Zhao, J. P. Xu, S. X. Hou, *Int. J. Pharm.* **2009**, *382*, 262–269.
[10] H. J. Song, C. Su, W. Y. Cui, B. Y. Zhu, L. W. Liu, Z. H. Chen, L. Zhao, *Biomed. Res. Int.* **2013**, 723158.
[11] Z. L. Wang, B. Xu, L. Zhang, J. B. Zhang, T. H. Ma, J. B. Zhang, X. Q. Fu, W. J. Tian, *Nanoscale* **2013**, *5*, 2065–2072.
[12] Y. C. Song, W. Shi, W. Chen, X. H. Li, H. M. Ma, *J. Mater. Chem.* **2012**, *22*, 12568–12573.
[13] W. Pan, H. J. Yang, T. T. Zhang, Y. H. Li, N. Li, B. Tang, *Anal. Chem.* **2013**, *85*, 6930–6935.
[14] S. N. Baker, G. A. Baker, *Angew. Chem. Int. Ed.* **2010**, *49*, 6726–6744; *Angew. Chem.* **2010**, *122*, 6876–6896.
[15] S. Nandi, R. Malishev, K. P. Kootery, Y. Mirsky, S. Kolusheva, R. Jelinek, *Chem. Commun.* **2014**, *50*, 10299–10302.
[16] S. K. Bhunia, A. Saha, A. R. Maity, S. C. Ray, N. R. Jana, *Sci. Rep.* **2013**, *3*, 1473.
[17] S. K. Bhunia, N. Pradhan, N. R. Jana, *ACS Appl. Mater. Interfaces* **2014**, *6*, 7672–7679.
[18] S. Nandi, M. Ritenberg, R. Jelinek, *Analyst* **2015**, *140*, 4232–4237.
[19] S. T. Yang, L. Cao, P. G. J. Luo, F. S. Lu, X. Wang, H. F. Wang, M. J. Mezzani, Y. F. Liu, G. Qi, Y. P. Sun, *J. Am. Chem. Soc.* **2009**, *131*, 11308–11309.
[20] Y. Suda, T. Ono, M. Akazawa, Y. Sakai, J. Tsujino, N. Homma, *Thin Solid Films* **2002**, *415*, 15–20.
[21] H. P. Liu, T. Ye, C. D. Mao, *Angew. Chem. Int. Ed.* **2007**, *46*, 6473–6475; *Angew. Chem.* **2007**, *119*, 6593–6595.
[22] M. E. Fortunato, M. Rostam-Abadi, K. S. Suslick, *Chem. Mater.* **2010**, *22*, 1610–1612.
[23] J. Jiang, Y. He, S. Y. Li, H. Cui, *Chem. Commun.* **2012**, *48*, 9634–9636.
[24] H. Li, W. Q. Kong, J. Liu, N. Y. Liu, H. Huang, Y. Liu, Z. H. Kang, *Carbon* **2015**, *91*, 66–75.
[25] H. Li, J. Liu, S. J. Guo, Y. L. Zhang, H. Huang, Y. Liu, Z. H. Kang, *J. Mater. Chem. B* **2015**, *3*, 2378–2387.
[26] H. Li, W. Q. Kong, J. Liu, M. M. Yang, H. Huang, Y. Liu, Z. H. Kang, *J. Mater. Chem. B* **2014**, *2*, 5652–5658.
[27] W. Q. Kong, R. H. Liu, H. Li, J. Liu, H. Huang, Y. Liu, Z. H. Kang, *J. Mater. Chem. B* **2014**, *2*, 5077–5082.
[28] L. B. Tang, R. B. Ji, X. K. Cao, J. Y. Lin, H. X. Jiang, X. M. Li, K. S. Teng, C. M. Luk, S. J. Zeng, J. H. Hao, S. P. Lau, *ACS Nano* **2012**, *6*, 5102–5110.
[29] P. Dubey, K. M. Tripathi, S. K. Sonkar, *RSC Adv.* **2014**, *4*, 5838–5844.
[30] S. J. Zhuo, M. W. Shao, S. T. Lee, *ACS Nano* **2012**, *6*, 1059–1064.
[31] S. H. Cho, S. Krishnan in *Cancer Nanotechnology: Principles and Applications in Radiation Oncology* (Eds.: William R. Hendee), Taylor and Francis, Boca Raton, **2013**.
[32] N. Tyagi, P. C. Ghosh, *Eur. J. Pharm. Sci.* **2011**, *43*, 343–353.

Manuscript received: December 26, 2015

Accepted article published: January 15, 2016

Final article published: February 24, 2016